JOURNAL OF CHEMICAL & ENGINEERING DATA

ARTICLE

pubs.acs.org/jced

An Ideal Absorbed Solution Theory (IAST) Study of Adsorption Equilibria of Binary Mixtures of Methane and Ethane on a Templated Carbon

Jiahui Chen,[†] Leslie S. Loo,[†] and Kean Wang*[,†,‡]

[†]School of Chemical and Biomedical Engineering, Nanyang Technological University, Singapore 637459

[‡]Department of Chemical Engineering, The Petroleum Institute, Abu Dhabi, United Arab Emirates

ABSTRACT: The adsorption equilibria of pure methane and ethane gases as well as their binary mixtures were measured on a template-synthesized carbon. The pure component isotherm data were fitted to the Sips equation, while the binary equilibria were studied by the extended Sips equation as well as the ideal adsorbed solution theory (IAST). It was found that the IAST performed better than the extended Sips in predicting the binary data on the highly heterogeneous carbon sample.

INTRODUCTION

In 1965, Prausnitz and Myers pioneered the work of ideal adsorbed solution theory or IAST in the article entitled "Thermodynamics of mixed-gas adsorption".[1] It quickly became a classic in the history of adsorption science and ranked No. 8 in the list of the most cited papers (a direct citation of 830+ is reported on ISI by Oct., 2010) in *AIChE Journal*'s 50 year history.[2] On the same list, Prausnitz's other three works on thermodynamics ranked No. 2,[3] No. 3,[4] and No. 4,[5] respectively.

IAST has been frequently used as the benchmark to evaluate experimental data and to validate new theories for adsorption equilibria of gas mixtures. On the basis of solution thermodynamics, IAST is a predictive model which does not require any mixture data and is independent of the actual model of physical adsorption.[6] Because of the thermodynamic consistency, it has been used to study adsorption equilibria for gas mixtures which are ideal or nonideal and on surfaces which are homogeneous or heterogeneous.[7,8] It was also successfully extended to the adsorption of mixed organic/inorganic solutes in aqueous solutions.[9,10] Reviews on the theory, its development, and applications are available in a few publications.[11−14]

Template synthesis is popularly used in synthesizing carbon adsorbents with regular porous structure. By depositing carbon sources (e.g., polymers or hydrocarbon gases) into the microchannels or pores of the template materials (e.g., zeolite, silica, etc.), the derived activated carbons (also referred to as the templated carbon or TC) possess the structural characteristics of the template.[15] In some cases, high-quality microporous replicas resembling the structural periodicity of the template can be obtained, and this type of TC is termed "ordered microporous carbon" or OMC.[16]

With selected template materials, carbon source, and processing conditions, TC can present a very high surface area ($> 3000\ m^2 \cdot g^{-1}$), a good micropore volume ($> 1.5\ cm^3 \cdot g^{-1}$), and a relatively homogeneous microporous structure with the pore sizes distributed around 1.0 nm. Such activated carbons are excellent candidates for the adsorptive storage of energy gases such as methane and hydrogen.

This research will report the adsorption of methane, ethane, and their binary mixtures on a TC. IAST was used to study the binary equilibria and compared to another model.

EXPERIMENTS

The ammonium-form zeolite Y (SiO_2/Al_2O_3 = 5.1) was impregnated with sucrose at room temperature. The mixture was dried and pyrolyzed at 1100 °C in a N_2 flow. An acid wash was then used to remove the template zeolite. The TC powder was obtained after washing, filtration, and drying.[17,18]

The N_2 isotherm was measured on the TC sample using a pore and surface analyzer (Quantachrome, Autosorb-1) at 77 K. Pure component isotherms of methane (C_1) and ethane (C_2) gases were measured on a volumetric rig fabricated with Swagelok parts.[19] Binary adsorption equilibria were obtained using a fixed bed rig operated at atmospheric pressure.[20,21] The details of the sample preparation, characterization, and experimental procedures are available in the references.[18,20,21]

THEORY

IAST is analogous to Raoult's law for vapor−liquid equilibrium, i.e.:

$$P_i = P_i^0(\pi_i)x_i \tag{1}$$

where x_i and π^i are the molar fraction and spreading pressure of component i in the adsorbed phase, respectively. At the adsorption equilibrium, the reduced spreading pressures must be the same for each component and the mixture:

$$\pi_i^* = \frac{\pi_i}{RT} = \int_0^{P_i^0} \frac{n_i^0(P)}{P}\,dP \qquad i = 1, 2, 3, \ldots, N \tag{2}$$

$$\pi_1^* = \pi_2^* = \ldots = \pi_N^* = \pi^* \tag{3}$$

The function $n^0{}_i(P)$ is the pure component equilibrium capacity and $P^0{}_i$ is the pure component hypothetical pressure which yields the same spreading pressure as that of the mixture.

Special Issue: John M. Prausnitz Festschrift

Received: October 26, 2010
Accepted: February 18, 2011
Published: March 03, 2011

By assuming ideal mixing at constant π and T, the total amount adsorbed, n_t, is:

$$\frac{1}{n_t} = \sum_{i=1}^{N} \left[\frac{x_i}{n_i^0(P_i^0)} \right] \quad (4)$$

with the constraint:

$$\sum_{i=1}^{N} x_i = 1 \quad (5)$$

Since the equations are nonlinear and the integrals in eq 2 cannot be solved analytically for most of the pure component isotherm equations, the classical IAST needs iterative integration processes. To cope with this issue, O'Brien and Myer developed a scheme (fast IAS or FASTIAS) for the rapid computation of multicomponent adsorption equilibria using IAST.[22]

The Sips isotherm is popularly used in the study of adsorption of pure component gases onto a heterogeneous surface:

$$\theta = \frac{(bP)^{1/n}}{1 + (bP)^{1/n}} \quad (6)$$

where θ is the surface coverage, b is the adsorption affinity, and n is the surface heterogeneity. The Sips isotherm can be directly extended to a multicomponent system with the format of:[23]

$$\theta_i = \frac{(b_i P_i)^{1/n}}{1 + \sum_{K=1}^{N} (b_k P_k)^{1/n}} \quad (7)$$

where N is the number of components in the system.

The IAST and the extended Sips isotherm model will be used to study the binary adsorption equilibria of C_1/C_2 measured on a templated carbon at 273 K.

RESULTS AND DISCUSSION

The pore size distributions of the TC were derived from the N_2 isotherm at 77 K (for pores ≥ 1.0 nm) and CO_2 isotherm at 273 K (for pores < 1.0 nm)[19] and were combined together in a bar chart, as shown in Figure 1. TC is seen to be predominantly microporous with the major micropore peak at 1.1 nm. A minor micropore peak was observed at ~0.8 nm, while broad mesopore peaks were identified in the size range of (2.5 to 4.0) nm. Other properties of the TC include a specific surface area of 1500 $m^2 \cdot g^{-1}$ and a micropore volume of 0.8 $cm^3 \cdot g^{-1}$.[19] Because of the difference in their molecular weights and dimensions (C_1: 0.38 nm; C_2: 0.39 nm), the adsorption potentials of C_1 and C_2 will vary greatly in small pores (< 1.0 nm) and are very different in big pores (e.g., (1.1 to 2.0) nm). The interaction energy between C_1 and C_2 for the competitive adsorption in a local pore can be related to their respective adsorption potentials in the pore, while the size exclusion effect may play an important role in small micropores.[20,21] The scanning electron microscopy (SEM) image of the TC, shown as an inset in Figure 1, indicates that the TC has a layered structure in its graphite crystals. All of the observations suggest that the TC presents strong surface heterogeneity toward the adsorption of C_1 and C_2 molecules.

Figure 2a and b shows the isotherm data of pure component C_1 and C_2 measured on the TC at three different temperatures. The adsorption capacities of C_1/C_2 are comparable to those of commercial Ajax carbon (with a surface area of 1200 $m^2 \cdot g^{-1}$ and

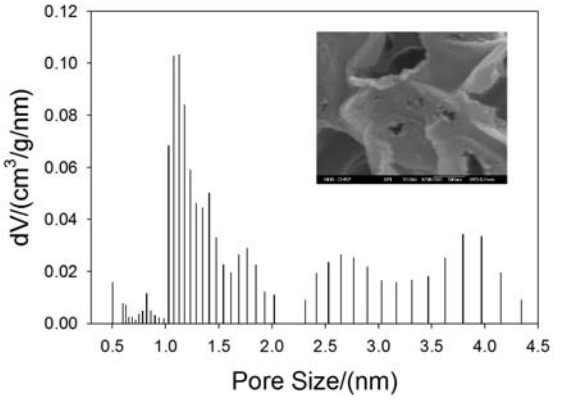

Figure 1. Schematic pore size distribution and the SEM image (inset) of the TC.

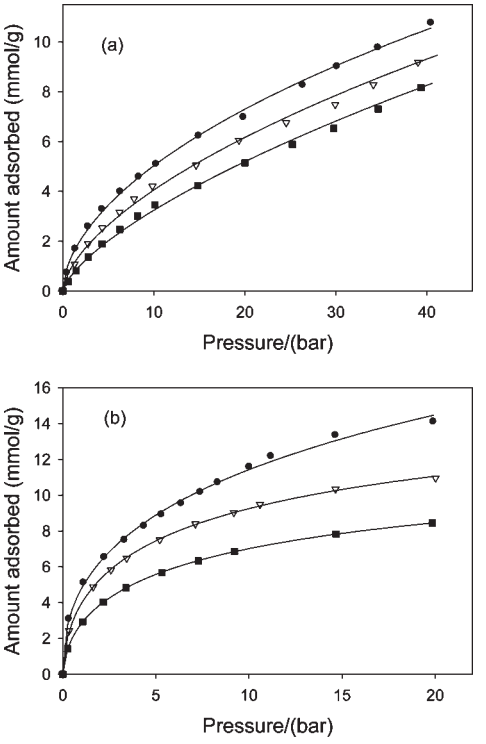

Figure 2. Adsorption isotherms on the TC and the fittings of Sips equation: (a) methane, (b) ethane. (●, 263 K; ▽, 273 K; ■, 303 K; —, Sips equation).

consisting of both micropores and mesopores) at the adsorption pressure of 1 bar.[8] As the TC is predominantly microporous and presents strong surface heterogeneity toward C_1 and C_2, the three-parametered Sips isotherm equation (eq 6) was used to fit the isotherm data of each component. The optimal fittings of the Sips equation are shown in Figure 2a and b as lines while the fitted isotherm parameters are listed in Table 1. The fittings are observed to be good for both species at all three temperatures. The values of the heterogeneity parameter n of the Sips equation are in agreement with our observations in Figure 1 that the TC has a highly heterogeneous surface.

The binary adsorption equilibria of C_1 and C_2 were measured on the TC at 273 K and under a total pressure of 1 bar. The experimental data (symbols) are presented in Figure 3 versus the

dx.doi.org/10.1021/je101099c |J. Chem. Eng. Data 2011, 56, 1209–1212

Table 1. Optimal Sips Isotherm Parameters of C_1/C_2 on the TC

	$C_{\mu s}$	b		T
	mmol·g^{-1}	bar^{-1}	n	K
methane	153.8	$2.36 \cdot 10^{-4}$	1.784	263
	454.5	$2.61 \cdot 10^{-5}$	1.769	273
	241.2	$1.99 \cdot 10^{-4}$	1.448	303
ethane	62.22	$3.19 \cdot 10^{-3}$	2.309	263
	18.66	$9.70 \cdot 10^{-2}$	1.769	273
	14.23	$9.52 \cdot 10^{-2}$	1.684	303

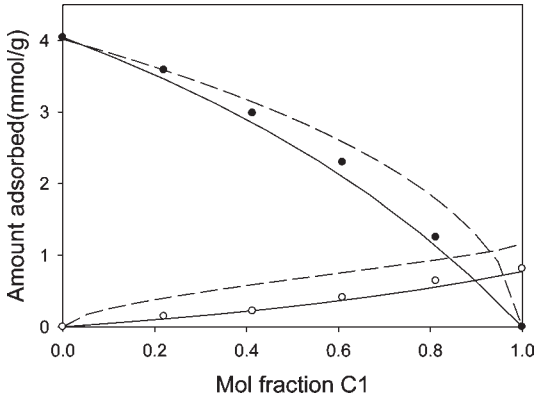

Figure 3. Binary adsorption equilibria of C_1 and C_2 on the TC at 273 K and 1 atm. (- - -, extended Sips model of eq 7; —, IAST model of eqs 1 to 5).

molar fraction of C_1 in the bulk phase. It is seen that, as the molar fraction (or the partial pressure) of C_1 increases, the adsorbed amount increases slowly for C_1 but decreases quickly for C_2. The binary equilibria data are listed in the Appendix, together with the isotherm data of pure C_1 and C_2.

Next, the extended Sips isotherm model [eq 7] was used to predict the binary data of C_1-C_2, based on the pure component isotherm parameters of C_1 and C_2 listed in Table 1. To keep the thermodynamic consistency of the model, the value of n in eq 6 was set to be the same for C_1 and C_2 at the temperature of 273 K. Such a constraint was seen to affect the value of the other fitted isotherm parameters of C_1 (i.e., a higher saturation capacity of $C_{\mu s}$ and a lower affinity of b); however, the goodness of fit of the Sips model was not affected, as shown in Figure 2.

The prediction results of the extended Sips equation are plotted in Figure 3 as dashed lines. The model correctly follows the trend of the experimental data but with large deviations. The average relative error (ARE)[8] of the prediction is 78 % for C_1 and 10 % for C_2. This is not surprising, as has been pointed out by Rudzinski et al.[23] that such a direct extension of the Sips equation is only applicable to the special case that the adsorption energy of each species are unrelated. In our TC sample, however, this is invalid as the TC possesses a range of micropores in which C_1 and C_2 will strongly adsorb and compete with each other. The interaction energies between the two species also vary significantly in pores of different sizes.[20] This explains the poor performance of the extended Sips model.

Next, IAST was invoked to simulate the binary data with the pure component isotherm parameters listed in Table 1. The simulation results are shown in Figure 3 as solid lines. We see that the IAST prediction is much better than the extended Sips model, with the ARE of 8.3 % and 4.6 % for C_1 and C_2, respectively. This is expected, because the performance of IAST only depends on the quality of the pure isotherm data of each species and is independent of the assumptions/theories underlining the isotherm model (e.g., the actual distribution of adsorption energy, etc.). The effect of adsorption energetic heterogeneity can also be taken into account by the heterogeneous IAST or HIAST, in which the overall adsorption equilibria is the integral of local equilibria on each energetic site which are evaluated individually by IAST. The application of IAST in this manner has been reported to improve the predictability in a few cases[7,8,13] but should be used with care, as it significantly increases the computation effort and requires a scheme to match the adsorption energies between different species on a local adsorption site.[20,21]

CONCLUSIONS

The ideal adsorbed solution theory was successfully applied to simulate the binary adsorption equilibria of methane and ethane on a template-synthesized carbon with strong surface heterogeneity. The prediction of IAST is found superior to the extended Sips model, which supports the underlining theory of IAST and its future application in the area of energy gas storage.

APPENDIX

Table A1. Adsorption Isotherm of Pure Methane/Ethane on the TC

P	n	P	n	P	n
bar	mmol·g^{-1}	bar	mmol·g^{-1}	bar	mmol·g^{-1}
		Methane			
263 K		273 K		303 K	
0.4600	0.7417	0.5070	0.4429	0.6120	0.3688
1.362	1.705	1.318	1.085	1.482	0.8079
2.779	2.594	2.772	1.901	2.819	1.368
4.312	3.287	4.338	2.533	4.329	1.895
6.312	3.995	6.241	3.162	6.276	2.477
8.340	4.592	7.839	3.697	8.203	3.016
10.25	5.103	9.849	4.209	10.13	3.463
14.92	6.234	14.66	5.052	14.84	4.230
19.84	6.989	19.35	6.043	20.01	5.143
26.34	8.282	24.56	6.754	25.24	5.890
30.12	9.023	29.93	7.489	29.78	6.533
34.64	9.781	34.13	8.279	34.64	7.307
40.44	10.77	39.04	9.184	39.36	8.164
		46.20	10.16	45.23	8.981
		Ethane			
0.3290	3.090	0.3420	2.421	0.2640	1.429
1.117	5.121	1.636	4.874	1.074	2.923
2.230	6.547	2.588	5.820	2.182	4.026
3.310	7.509	3.438	6.481	3.397	4.832
4.360	8.280	5.217	7.511	5.327	5.678
5.303	8.930	7.132	8.396	7.285	6.329

Table A1. Continued

P	n	P	n	P	n
bar	mmol·g^{-1}	bar	mmol·g^{-1}	bar	mmol·g^{-1}
6.365	9.551	9.195	9.031	9.226	6.857
7.385	10.18	10.59	9.482	14.67	7.828
8.321	10.72	14.65	10.34	19.84	8.439
10.01	11.59	20.02	10.96		
19.90	14.11				

Table A2. Equilibria of Binary Mixture of Methane/Ethane at 273 K, 1 atm

	C_2	C_1
C_1-Yi	mmol·g^{-1}	mmol·g^{-1}
0.000	4.040	0.000
0.2200	3.587	0.1456
0.4130	2.985	0.2214
0.6090	2.298	0.4090
0.8120	1.253	0.6432
1.000	0.000	0.8123

AUTHOR INFORMATION

Corresponding Author

*E-mail: mkwang@ntu.edu.sg.

REFERENCES

(1) Myers, A. L.; Prausnitz, J. M. Thermodynamics of mixed-gas adsorption. *AIChE J.* **1965**, *11* (1), 121–127.

(2) The 100 most cited articles in AIChE Journal history. *AIChE J.* **2004**, *50*, (1), 4−6.

(3) Renon, H.; Prausnitz, J. M. Local compositions in thermodynamic excess functions for liquid mixtures. *AIChE J.* **1968**, *14* (1), 135–144.

(4) Abrams, D. S.; Prausnitz, J. M. Statistical thermodynamics of liquid mixtures: A new expression for the excess Gibbs energy of partly or completely miscible systems. *AIChE J.* **1975**, *21* (1), 116–128.

(5) Fredenslund, A.; Jones, R. L.; Prausnitz, J. M. Group-contribution estimation of activity coefficients in nonideal liquid mixtures. *AIChE J.* **1975**, *21* (6), 1086–1099.

(6) O'Brien, J. A.; Myers, A. L. Rapid calculations of multicomponent adsorption equilibria from pure isotherm data. *Ind. Eng. Chem. Process Des. Dev.* **1985**, *24* (4), 1188–1191.

(7) O'Brien, J. A.; Myers, A. L. Physical adsorption of gases on heterogeneous surfaces. Series expansion of isotherms using central moments of the adsorption energy distribution. *J. Chem. Soc., Faraday Trans. 1* **1984**, *80* (6), 1467–1477.

(8) Ahmadpour, A.; Wang, K.; Do, D. D. Comparison of models on the prediction of binary equilibrium data of activated carbons. *AIChE J.* **1998**, *44* (3), 740–752.

(9) Vijayaraghavan, K.; Yun, Y.-S. Bacterial biosorbents and biosorption. *Biotechnol. Adv.* **2008**, *26* (3), 266–291.

(10) Cheung, C. W.; Ko, D. C. K.; Porter, J. F.; McKay, G. Binary Metal Sorption on Bone Char Mass Transport Model Using IAST. *Langmuir* **2003**, *19* (10), 4144–4153.

(11) Ruthven, D. M. *Principles of adsorption and adsorption processes*; John Wiley & Sons: New York, 1984; Vol. 7.

(12) Prausnitz, J. M.; Lichtenthaler, R. N.; Gomes de Azevedo, E. *Molecular thermodynamics of fluid-phase equilibria*, 3rd ed.; Prentice-Hall: Upper Saddle River, NJ, 1999.

(13) Diego, P.; Valenzuela, A. L. M. *Adsorption equilibrium data handbook*; Prentice-Hall: Englewood Cliffs, NJ, 1989.

(14) Myers, A. L. Thermodynamics of adsorption. In *Chemical thermodynamics for industry*; Letcher, T. M., Ed.; Royal Society of Chemistry: Cambridge, UK, 2004.

(15) Kyotani, T.; Nagai, T.; Inoue, S.; Tomita, A. Formation of New Type of Porous Carbon by Carbonization in Zeolite Nanochannels. *Chem. Mater.* **1997**, *9* (2), 609–615.

(16) Ma, Z.; Kyotani, T.; Tomita, A. Synthesis methods for preparing microporous carbons with a structural regularity of zeolite Y. *Carbon* **2002**, *40* (13), 2367–2374.

(17) Su, F.; Lv, L.; Hui, T. M.; Zhao, X. S. Phenol adsorption on zeolite-templated carbons with different structural and surface properties. *Carbon* **2005**, *43* (6), 1156–1164.

(18) Guan, C.; Su, F.; Zhao, X. S.; Wang, K. Methane storage in a template-synthesized carbon. *Sep. Purif. Technol.* **2008**, *64* (1), 124–126.

(19) Guan, C.; Wang, K.; Yang, C.; Zhao, X. S. Characterization of a zeolite-templated carbon for H2 storage application. *Microporous Mesoporous Mater.* **2009**, *118* (1−3), 503–507.

(20) Wang, K.; Qiao, S.; Hu, X. Application of IAST in the Prediction of Multicomponent Adsorption Equilibrium of Gases in Heterogeneous Solids: Micropore Size Distribution versus Energy Distribution. *Ind. Eng. Chem. Res.* **1999**, *39* (2), 527–532.

(21) Wang, K.; Qiao, S.; Hu, X. On the performance of HIAST and IAST in the prediction of multicomponent adsorption equilibria. *Sep. Purif. Technol.* **2000**, *20* (2−3), 243–249.

(22) O'Brien, J. A.; Myers, A. L. A comprehensive technique for equilibrium calculations in adsorbed mixtures: the generalized FastIAS method. *Ind. Eng. Chem. Res.* **1988**, *27* (11), 2085–2092.

(23) Rudzinski, W.; Nieszporek, K.; Moon, H.; Rhee, H.-K. On the theoretical origin and applicability of the potential theory approach to predict mixed-gas adsorption on solid surfaces from single-gas adsorption isotherms. *Chem. Eng. Sci.* **1995**, *50* (16), 2641–2660.